BUTTERWORTH HEINEMANN

Polymer Vol. 36 No. 5, pp. 1097–1107, 1995

0032-3861/95/$10.00 + 0.00

Synthesis and characterization of polymer precursors bearing 2,2-dicyanovinyl groups and their curing to thermally stable and electrically conductive resins

Constantinos D. Diakoumakos and John A. Mikroyannidis*
Department of Chemistry, University of Patras, GR-26500 Patras, Greece

and Christoforos A. Krontiras and Michael N. Pisanias
Department of Physics, University of Patras, GR-26500 Patras, Greece
(Received 1 June 1994)

4-Carboxybenzaldehyde was condensed with malononitrile to afford 1-(2,2-dicyanovinyl)-4-benzoic acid, which was converted to the corresponding acid chloride. The latter reacted with half the molar amount of an aromatic diamine or bisphenol to yield cyano-substituted polymer precursors. Crosslinked polymers were obtained by curing at 300°C for 40–60 h, which were stable up to 333–400°C in N_2 or air and afforded anaerobic char yield of 35–60% at 800°C. Prior to pyrolysis all polymer precursors are of amorphous structure and behave, at room temperature, as insulators. A dramatic decrease of the electrical resistivity is observed with increasing pyrolysis temperature. All resulting conductive materials exhibited crystalline structure revealed by their X-ray diffraction profiles. The temperature dependence of the electrical resistivity in the range −173 to 327°C (100 to 600 K) of all pyrolysed materials suggests that they have semiconducting properties. The variable-range hopping model as well as a thermally activated conduction model were applied in order to interpret the experimental data. The observed electrical conductivity seems to be thermally activated and may be associated with intermolecular and intramolecular hopping conduction processes. The activation energies for the intermolecular process range from 0.265 to 0.012 eV and for the intramolecular process from 0.380 to 0.047 eV, depending on the pyrolysis temperature. The electrical behaviour of all conductive materials can be easily controlled, from insulating to semiconducting, by controlling both the pyrolysis temperature and duration. The highest electrical conductivity of 20 S cm^{-1} has been obtained for two samples pyrolysed at 800°C for 40 h.

(Keywords: thermally stable resins; cyano-substituted monomers; conductive polymers)

INTRODUCTION

Oligomers with terminal groups that undergo thermally induced crosslinking or chain extension reactions without evolving volatile by-products are good precursors for high-performance polymers and composite matrices[1].

It is well established[2–4] that the electronic structure of polymers is such that electrical conduction occurs along the unsaturated π-bonds. Therefore, pyrolysis of polymers, under vacuum or inert atmosphere, at temperatures higher than the curing temperature introduces changes in the π-electron system that affect the electrical conductivity. As a polymer is pyrolysed, planar polycondensed rings are developed, which result in the progressive increase in conjugation and π-orbital delocalization.

Certain new cyano-substituted polyamides and polyimides have recently been prepared and crosslinked in our laboratory. More particularly, some polyamides containing enaminonitrile segments[5,6], *N*-cyano-substituted polyamides[7] and polyamides bearing pendent cyano groups derived from 1,4-bis(2-cyano-2-carboxyvinyl)benzene[8], 1-carboxy-4-(2-cyano-2-carboxyvinyl)benzene[9] as well as cyano-substituted polyamides and polyimides prepared from 2,6-bis(3-aminobenzylidene)-1-dicyanomethylenecyclohexane[10] and 2,7-diamino-9-dicyanomethylenefluorene[11] have been synthesized. In addition, we have reported the synthesis of cyano-substituted polyester derived from 2,6-bis(4-hydroxybenzylidene)-1-dicyanomethylenecyclohexane[12]. Furthermore, some polymer precursors bearing 2,2-dicyanovinyl terminal groups have recently been synthesized and crosslinked[13].

The subject of the present investigation is the synthesis, characterization and study of the electrical conductivity of a new series of diamide and diester polymer precursors terminated with 2,2-dicyanovinyl groups. Upon heat curing at 300°C in static air, these precursors afforded thermally stable resins without the evolution of volatile by-products. Following pyrolysis in inert atmosphere, they yielded conductive materials at temperatures higher than 500°C.

In order to elucidate the effect of substituents on the electrical conduction mechanisms of the synthesized diamides and diesters, the electrical resistivity of the

* To whom correspondence should be addressed

resulting material, following pyrolysis, was studied as a function of temperature and pyrolysis duration.

EXPERIMENTAL

Characterization methods

Melting temperatures were determined on an electrothermal melting-point apparatus IA6304 and are uncorrected. *FT*i.r. spectra were recorded on a Perkin–Elmer 16PC *FT*i.r. spectrometer with KBr pellets. ^{1}H n.m.r. spectra were obtained using a Varian T-60A spectrometer at 60 MHz. Chemical shifts (δ values) are given in parts per million with tetramethylsilane as an internal standard. Dynamic thermal analyses (d.t.a.) and thermogravimetric analyses (t.g.a.) were performed on a DuPont 990 thermal analyser system. D.t.a. measurements were made using a high-temperature (1200°C) cell in N_2 atmosphere at a flow rate of 60 cm^3 min^{-1}. Dynamic t.g.a. measurements were made at a heating rate of 20°C min^{-1} in atmospheres of N_2 or air at a flow rate of 60 cm^3 min^{-1}. Thermal studies were also carried out in static air with a heating rate of 5°C min^{-1} using the thermal mechanical analyser (t.m.a.), model 943, attached to a DuPont 2000 thermal analyser. Elemental analyses were carried out with a Hewlett–Packard model 185 analyser. The wide-angle X-ray diffraction patterns were obtained for powder specimens on a Philips PW-1840 X-ray diffractometer and the 2θ span was extended from 30° to 70°.

Reagents and solvents

4-Carboxybenzaldehyde and 4,4′-diaminodiphenyl ether as well as hydroquinone were recrystallized from acetonitrile. 4,4′-Diaminodiphenylmethane and 2,2′-bis(4-hydroxyphenyl)propane (bisphenol A) were recrystallized from toluene and ether, respectively. 1,4-Phenylenediamine was sublimed under reduced pressure (2–3 mm). Malononitrile and thionyl chloride were used as supplied. 1,4-Dioxane, acetonitrile and acetone were purified by distillation. All reagents and solvents were obtained from Aldrich.

Synthesis of 1-(2,2-dicyanovinyl)-4-benzoyl chloride (DBC) (Scheme 1)

A mixture of 4-carboxybenzaldehyde (10.0000 g, 66.60 mmol), malononitrile (8.8000 g, 133.20 mmol), 1,4-dioxane (60 ml) and glacial acetic acid (5 ml) was refluxed for 24 h. It was subsequently concentrated under reduced pressure to remove about half of the solvent as well as volatile components and the residue was poured into water. The brown solid precipitate was filtered off, washed with water and dried to afford 1-(2,2-dicyanovinyl)-4-benzoic acid (DBA) (10.02 g, yield 76%). A purified sample with m.p. 193–196°C was obtained by recrystallization from 95% ethanol.

Analysis calculated for $C_{11}H_6N_2O_2$: C, 66.65%; H, 3.05%; N, 14.14%. Found: C, 66.11%; H, 3.06%; N, 13.85%.

I.r. (KBr) (cm^{-1}): 3036–2544 (O–H stretching); 2230 (C≡N); 1701 (C=O); 1591 (olefinic bond); 1560, 1507 (aromatic); 1424, 1293 (C–O and O–H deformation).

^{1}H n.m.r. (DMSO-d_6) δ (ppm): 8.90 (s, 1H, olefinic); 8.36 (s, 4H, aromatic). The carboxylic proton was unobserved.

A flask was charged with a solution of DBA (8.0000 g, 40.36 mmol) in acetonitrile (40 ml). Thionyl chloride (15 ml) and a catalytic amount of *N*,*N*-dimethylformamide (DMF) were added to the stirred solution. The mixture was refluxed for 40 min and it was subsequently concentrated under reduced pressure. The dark brown solid obtained was filtered off, washed with ether and dried to afford DBC (7.52 g, yield 86%). A purified sample obtained by recrystallization from toluene had m.p. 93–96°C (dec.).

Analysis calculated for $C_{11}H_5N_2OCl$: C, 61.11%; H, 2.33%; N, 12.97%. Found: C, 60.47%; H, 2.32%; N, 12.71%.

I.r. (KBr) (cm^{-1}): 2219 (C≡N); 1785, 1701 (C=O); 1591 (olefinic bond); 1560 (aromatic).

^{1}H n.m.r. (DMSO-d_6) δ (ppm): 8.96 (s, 1H, olefinic); 8.30 (s, 4H, aromatic).

Preparation of polymer precursors (Scheme 1)

Diamides DAM, DAO and DAP. A flask equipped with a dropping funnel and magnetic stirrer was charged with a solution of 4,4′-diaminodiphenylmethane (0.5472 g, 2.76 mmol) in acetone (5 ml), and triethylamine (0.5586 g, 5.52 mmol) was added to the solution. DBC (1.1961 g, 5.52 mmol) dissolved in acetone (10 ml) was added dropwise at 0°C under N_2. The mixture was subsequently stirred at ambient temperature for 3 h in a stream of N_2. The brown solid precipitate was filtered off, washed with water and dried to afford DAM (1.39 g, yield 90%). It was recrystallized from DMF (m.p. > 300°C).

Analysis calculated for $C_{35}H_{22}N_6O_2$: C, 75.24%; H, 3.97%; N, 15.05%. Found: C, 74.63%; H, 3.96%; N, 14.87%.

I.r. (KBr) (cm^{-1}): 3351 (N–H stretching); 2188 (C≡N); 1654 (C=O); 1602 (olefinic bond); 1554 (N–H deformation); 1513 (aromatic); 1413 (CH_2); 1324 (C–N stretching and N–H bending).

^{1}H n.m.r. (DMSO-d_6) δ (ppm): 11.51 (b, 2H, NHCO); 8.48–7.61 (m, 16H, aromatic and 2H, olefinic); 3.75 (s, 2H, CH_2).

Diamide DAO was similarly prepared as a brown solid in 93% yield (1.44 g) by reacting 4,4′-diaminodiphenyl ether (0.5542 g, 2.76 mmol) with DBC (1.1961 g, 5.52 mmol). A purified sample obtained by recrystallization from a mixture of DMF/water (1:1 v/v) had m.p. > 300°C.

Analysis calculated for $C_{34}H_{20}N_6O_3$: C, 72.84%; H, 3.60%; N, 15.00%. Found: C, 72.33%; H, 3.61%; N, 14.77%.

I.r. (KBr) (cm^{-1}): 3361 (N–H stretching); 2188 (C≡N); 1649 (C=O); 1612 (olefinic bond); 1539 (N–H deformation); 1497 (aromatic); 1319 (C–N stretching and N–H bending).

^{1}H n.m.r. (DMSO-d_6) δ (ppm): 11.35 (b, 2H, NHCO); 8.44–7.59 (m, 16H, aromatic and 2H, olefinic).

Diamide DAP was prepared in a similar manner from the reaction of 1,4-phenylenediamine (0.2992 g, 2.76 mmol) with DBC (1.1961 g, 5.52 mmol) as a brown solid (1.18 g, yield 91%). It was recrystallized from a mixture of DMF/water (1:2 v/v) and had m.p. > 300°C.

Analysis calculated for $C_{28}H_{16}N_6O_2$: C, 71.77%; H, 3.44%; N, 17.95%. Found: C, 71.16%; H, 3.42%; N, 17.71%.

I.r. (KBr) (cm^{-1}): 3361 (N–H stretching); 2188 (C≡N);

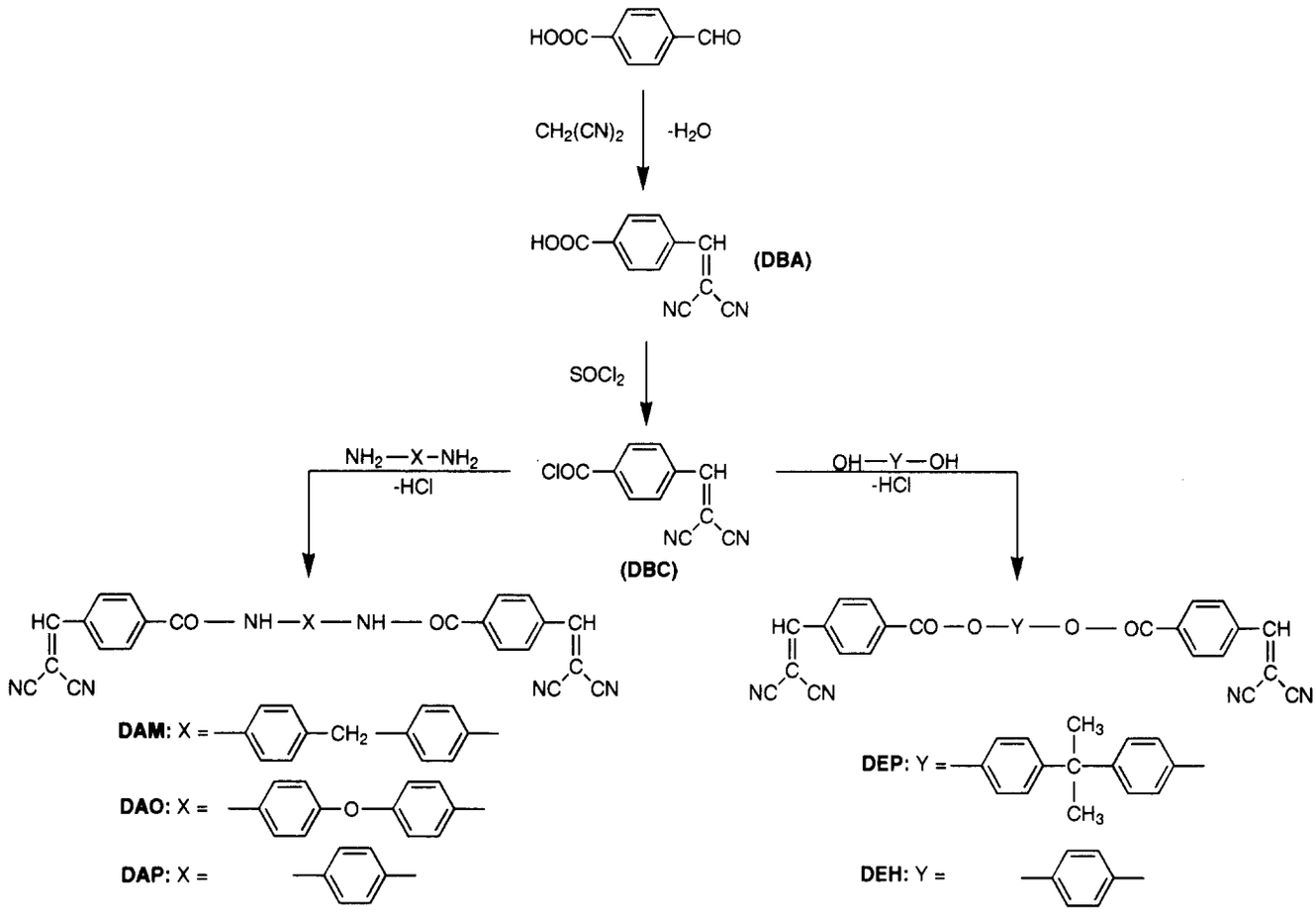

Scheme 1

1654 (C=O); 1612 (olefinic bond); 1544 (N–H stretching); 1513 (aromatic); 1319 (C–N stretching and N–H bending).

^{1}H n.m.r. (DMSO-d_6) δ (ppm): 11.21 (b, 2H, NHCO); 8.40–7.64 (m, 12H, aromatic and 2H, olefinic).

Diesters DEP and DEH. A flask was charged with a mixture of 2,2′-bis(4-hydroxyphenyl)propane (0.6320 g, 2.76 mmol), acetone (8 ml) and triethylamine (0.5586 g, 5.52 mmol). A solution of DBC (1.1961 g, 5.52 mmol) in acetone (10 ml) was added dropwise to the stirred solution at 0°C under N_2. Stirring of the mixture was continued at room temperature for 3 h in a stream of N_2. The brownish solid precipitate was filtered off, washed with water and dried to afford DEP (1.48 g, yield 91%). It was recrystallized from DMF (m.p. > 300°C).

Analysis calculated for $C_{37}H_{24}N_4O_4$: C, 75.49%; H, 4.11%; N, 9.52%. Found: C, 74.91%; H, 4.12%; N, 9.29%.

I.r. (KBr) (cm^{-1}): 2188 (C≡N); 1738 (C=O); 1612 (olefinic bond); 1507 (aromatic); 1272 (C–O–C stretching).

^{1}H n.m.r. (DMSO-d_6) δ (ppm): 8.31–7.40 (m, 16H, aromatic and 2H olefinic); 2.05 (s, 6H, CH_3).

Diester DEH was similarly prepared as a brownish solid in 92% yield (1.19 g) from the reaction of hydroquinone (0.3046 g, 2.76 mmol) with DBC (1.1961 g, 5.52 mmol). A purified sample obtained by recrystallization from a mixture of DMF/water (1:2 v/v) had m.p. > 300°C.

Analysis calculated for $C_{28}H_{14}N_4O_4$: C, 71.47%; H, 3.00%; N, 11.91%. Found: C, 70.91%; H, 2.99%; N, 11.72%.

I.r. (KBr) (cm^{-1}): 2188 (C≡N); 1732 (C=O); 1612 (olefinic bond); 1502 (aromatic); 1266 (C–O–C stretching).

^{1}H n.m.r. (DMSO-d_6) δ (ppm): 8.29–7.32 (m, 12H, aromatic and 2H, olefinic).

Preparation of thermosetting resins

Diamides DAM, DAE and DAP were placed separately in an aluminium dish and curing was accomplished by heating in an oven at 300°C for 40 h in static air. In the case of diesters DEP and DEH, curing was performed at 300°C for 60 h.

Preparation of pyrolysed conductive resins

All thermosetting resins were pressed to form pellets of 10 mm in diameter. Each pellet was then put in an alumina boat and pyrolysed in a quartz tube that was placed in a programmable furnace. After the preset pyrolysis temperature of 550, 700 or 800°C was reached, the resulting pellets were left in the oven for 10 h. During the entire pyrolysis duration nitrogen of extremely high purity (99.999%) was flowing through the quartz tube. The pyrolysis temperature was kept below 900°C in order to avoid graphitization of the polymers[14].

Following pyrolysis, each pellet was mounted on the sample holder of a cryostat and the electrical resistivity was measured as a function of temperature from −173 to 327°C (100 to 600 K) by applying the Van der Pauw method. Details regarding the resistivity measurements were presented elsewhere[15].

In order to study the effect of pyrolysis duration on

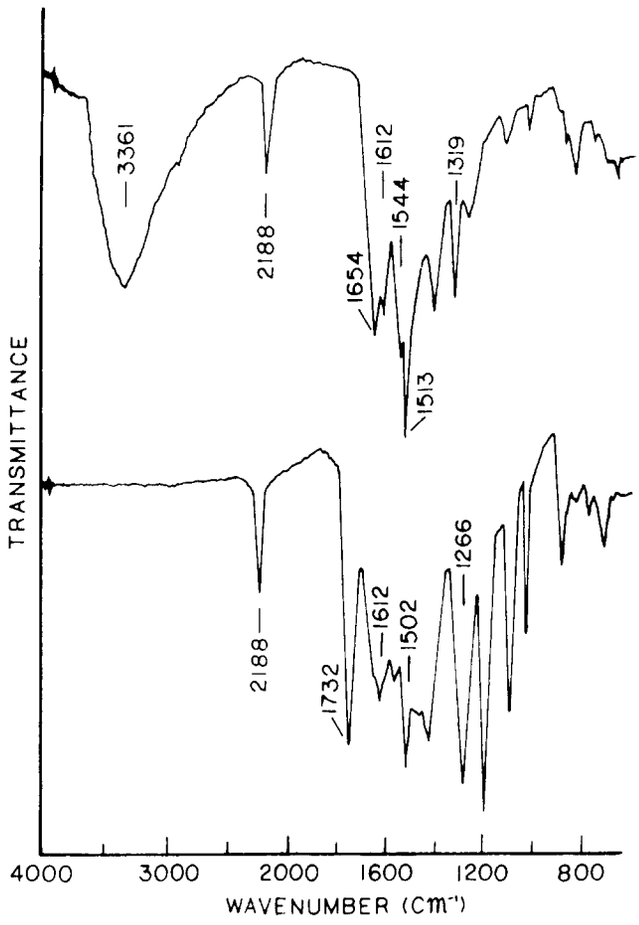

Figure 1 *FT*i.r. spectra of diamide DAP (top) and diester DEH (bottom)

the electrical conductivity, two pyrolysis temperatures were selected, specifically 550 and 800°C, and the pellets were pyrolysed for 10 to 40 h in steps of 10 h. The room-temperature electrical conductivity was then measured following every pyrolysis time interval.

The crystal structure of both the unpyrolysed (non-heat-treated (NHT)) and the resulting pyrolysed materials was examined by X-ray diffraction.

RESULTS AND DISCUSSION

Synthesis, characterization and curing of polymer precursors

Certain diamide and diester polymer precursors bearing 2,2-dicyanovinyl terminal groups were synthesized according to the chemical reactions of *Scheme 1*. More particularly, 4-carboxybenzaldehyde was condensed with malononitrile in the presence of glacial acetic acid to afford 1-(2,2-dicyanovinyl)-4-benzoic acid (DBA). The reaction was carried out in refluxing 1,4-dioxane and excess malononitrile was used to improve the reaction yield. DBA was converted to the corresponding acid chloride DBC by reacting with thionyl chloride. The diamide polymer precursors DAM, DAE and DAP were synthesized from the reactions of DBC with half the molar amount of 4,4′-diaminodiphenylmethane, 4,4′-diaminodiphenyl ether and 1,4-phenylenediamine, respectively, in the presence of triethylamine. The diester polymer precursors DEP and DEH were similarly prepared from the reactions of DBC with bisphenol A and hydroquinone, respectively.

All compounds were characterized by elemental analyses as well as *FT*i.r. and ^{1}H n.m.r. spectroscopy (see 'Experimental'). The reaction of 4-carboxybenzaldehyde with malononitrile could be monitored by ^{1}H n.m.r. spectroscopy because the aldehyde proton near $\delta = 10$ ppm gradually disappeared with the progress of the reaction. Note that the carboxylic proton of DBA was unobserved in its ^{1}H n.m.r. spectrum, probably due to exchange with the trace of moisture present in the solvent.

Upon gradual heating in a capillary tube, none of the polymer precursors showed a melting temperature. The formation of crosslinks during heating was responsible for this behaviour. In addition, the d.t.a. traces in N_2 of the polymer precursors did not display an endotherm associated with melting.

Figure 1 presents typical *FT*i.r. spectra of polymer precursors DAP and DEH. The former showed absorption bands assigned to the amide structure at 3361 (N–H stretching), 1654 (C=O), 1544 (N–H deformation) and 1319 cm^{-1} (C–N stretching and N–H bending). The latter displayed the characteristic absorptions of the ester structure at 1732 (C=O) and 1266 cm^{-1} (C–O–C stretching). Both compounds showed a sharp absorption at 2188 cm^{-1} attributable to the cyano groups.

The polymer precursors afforded heat-resistant thermosetting resins by heating in static air at 300°C; whereas on heating in inert atmosphere above 500°C, they yielded a conductive material (*Scheme 2*). The thermosetting resins possessed a network structure resulting from the thermally induced crosslinking reactions through the olefinic bonds as well as the cyano groups. To optimize the curing conditions with respect to the thermal stability of the resin obtained, two typical polymer precursors DAM and DEP were heated at 300°C for various periods and the initial decomposition temperature (*IDT*) and the char yield (Y_c) of the resulting resins at 800°C in N_2 were determined by t.g.a. (*Figure 2*). It is seen that both *IDT* and Y_c were enhanced with increased curing time up to 40 h for DAM and 60 h for DEP, and they were reduced beyond this time. Therefore, the time of 40 h and 60 h was selected for DAM and DEP, respectively, when curing was performed at 300°C.

The cured resins obtained from polymer precursors DAM, DAO and DAP upon curing at 300°C for 40 h as well as from DEP and DEH upon curing at 300°C for 60 h are referred to by the designations DAM′, DAO′, DAP′, DEP′, DEH′, respectively. Note that all cured

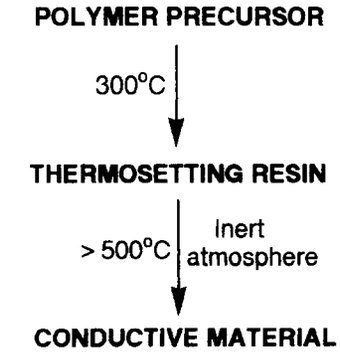

Scheme 2

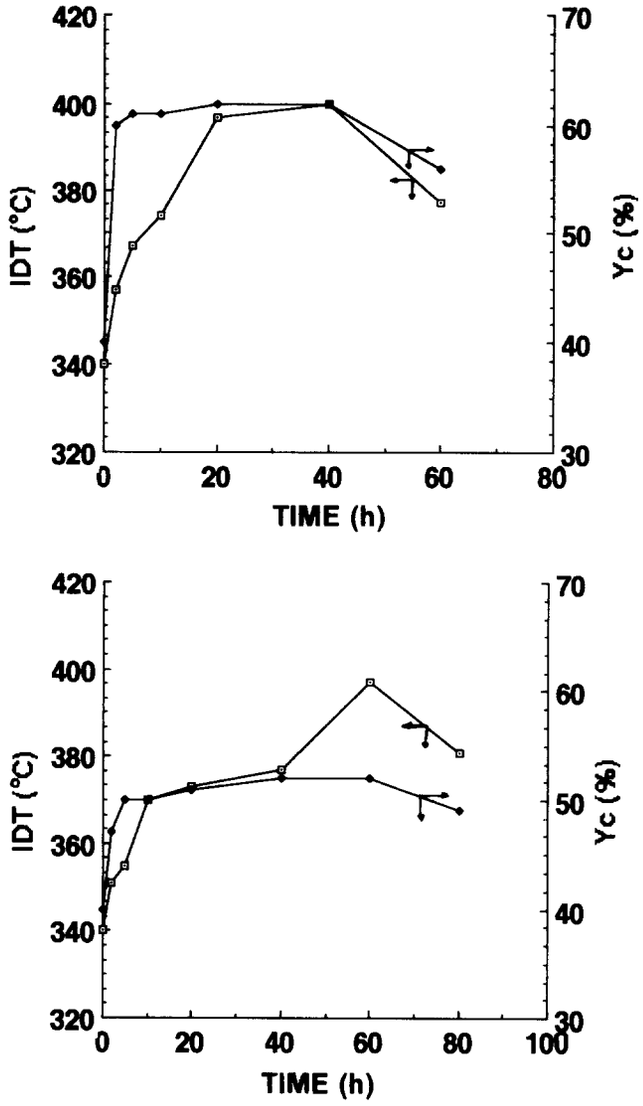

Figure 2 IDT and Y_c at 800°C in N_2 of diamide DAM (top) and diester DEP (bottom) as a function of the curing time at 300°C

resins were completely insoluble even in 98% H_2SO_4 and their FTi.r. spectra showed a remarkable reduction of the absorption band at 2188 cm^{-1} assigned to the cyano groups. The latter were consumed through the trimerization reaction, forming melamine and isomelamine rings[16]. The thermal stability of cured resins was ascertained by t.g.a. *Figure 3* shows typical t.g.a. traces in N_2 and air for cured resins DAM′ and DEP′. The IDT, the polymer decomposition temperature (PDT) and the maximum polymer decomposition (PDT_{max}) in both N_2 and air as well as the anaerobic Y_c at 800°C for all resins are summarized in *Table 1*. The IDT and PDT were determined as the temperature at which 0.5 and 10% weight loss was observed, respectively. PDT_{max} corresponds to the temperature at which the maximum rate of weight loss occurred. The cured resins were stable up to 333–400°C in N_2 or air and afforded anaerobic char yield of 35–60% at 800°C. The ratio IDT_{air}/IDT_{N_2} was 0.86–0.90. Thus, the thermal degradation of the resins was slightly affected by the presence of oxygen.

In addition, the glass transition (T_g) temperatures of the resins were determined by the thermal mechanical analysis (t.m.a.) method and they are listed in *Table 1*. The T_g values ranged from 211 to 303°C. The T_g values of diamide polymer precursors were higher than those of the diester ones, probably due to the formation of hydrogen bonds.

Electrical properties of pyrolysed resins

An attempt was made to elucidate the crystal structure by X-ray diffraction analysis of all monomers prior to pyrolysis as well as of the conductive materials obtained after the pyrolysis. *Figures 4* and *5* show the X-ray diffraction profiles of DAM, DAP, DEP and DEH, respectively, prior to pyrolysis and following pyrolysis at 550 and 800°C. The absence of any peaks in the X-ray diffractograms of all unpyrolysed monomers is profound. This reveals their amorphous state. Following pyrolysis at 550°C, all resulting conductive materials exhibited crystal ordering, as inferred by the appearance of the peaks recorded. The 2θ span was limited from 30° to 70° in order to exclude the sample holder contribution to the diffractogram. The transition from the amorphous to microcrystalline state as the pyrolysis temperature increases has been reported by others[17]. Comparing the X-ray diffractograms taken from samples pyrolysed at 550 and 800°C, it is evident that additional peaks were observed whereas others disappeared. This could be associated with the simultaneous formation of a new crystalline phase resulting in the presence of a multiphase system[18,19]. As the pyrolysis temperature increases, the

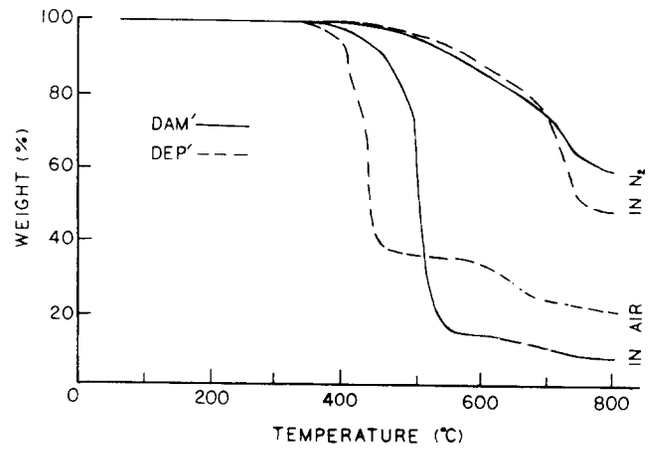

Figure 3 T.g.a. thermograms of cured resins DAM′ and DEP′ in N_2 and air. Conditions: gas flow 60 cm^3 min^{-1}; heating rate 20°C min^{-1}

Table 1 Thermal stabilities and T_g values of cured resins

		N_2				Air		
Sample	T_g[a] (°C)	IDT[b] (°C)	PDT[c] (°C)	PDT_{max}[d] (°C)	Y_c[e] (%)	IDT (°C)	PDT (°C)	PDT_{max} (°C)
DAM′	290	400	567	726	60	355	463	501
DAE′	260	397	533	720	45	359	456	486
DAP′	303	392	556	728	48	355	465	512
DEP′	211	397	589	730	52	340	419	456
DEH′	238	384	487	725	35	333	407	437

[a] Glass transition temperature determined by t.m.a. method
[b] Initial decomposition temperature
[c] Polymer decomposition temperature
[d] Maximum polymer decomposition temperature
[e] Char yield at 800°C

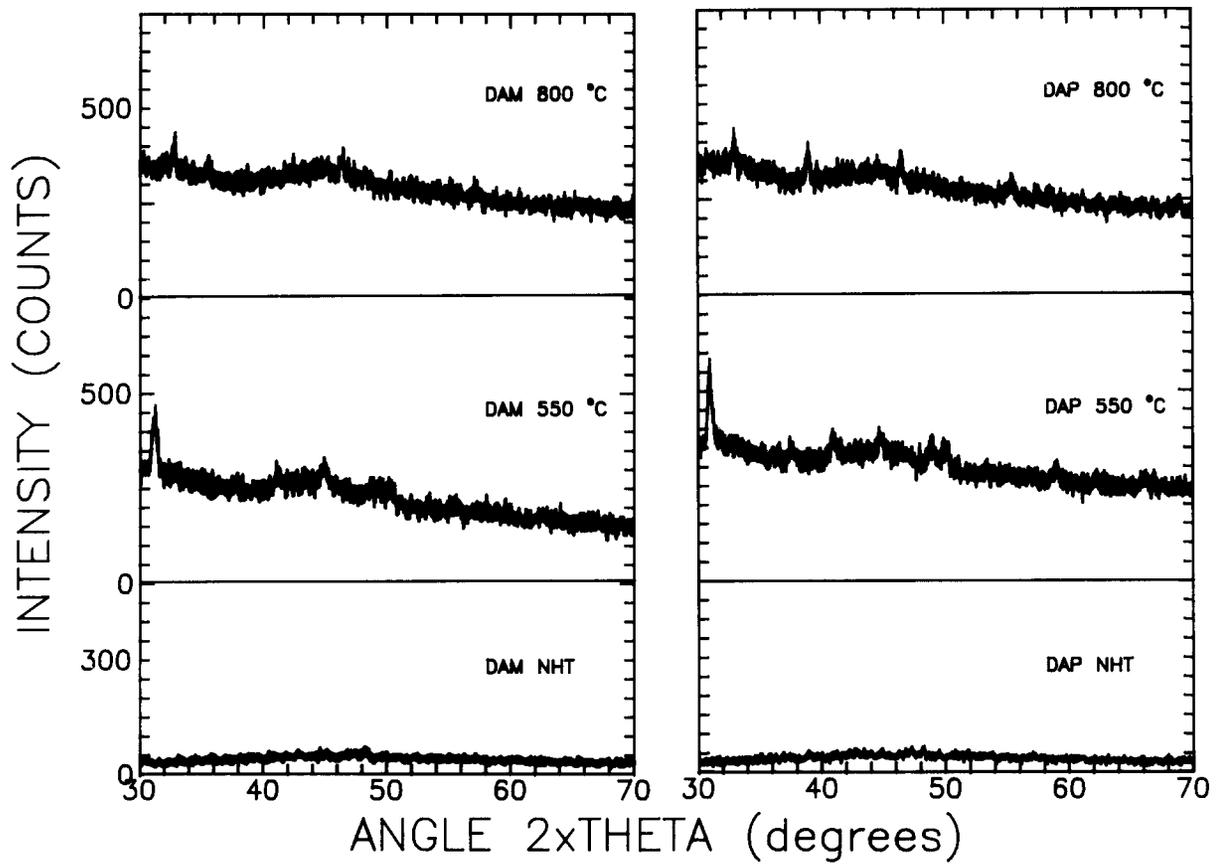

Figure 4 X-ray diffractograms of unpyrolysed DAM and DAP samples as well as of the conductive materials produced at 550 and 800°C

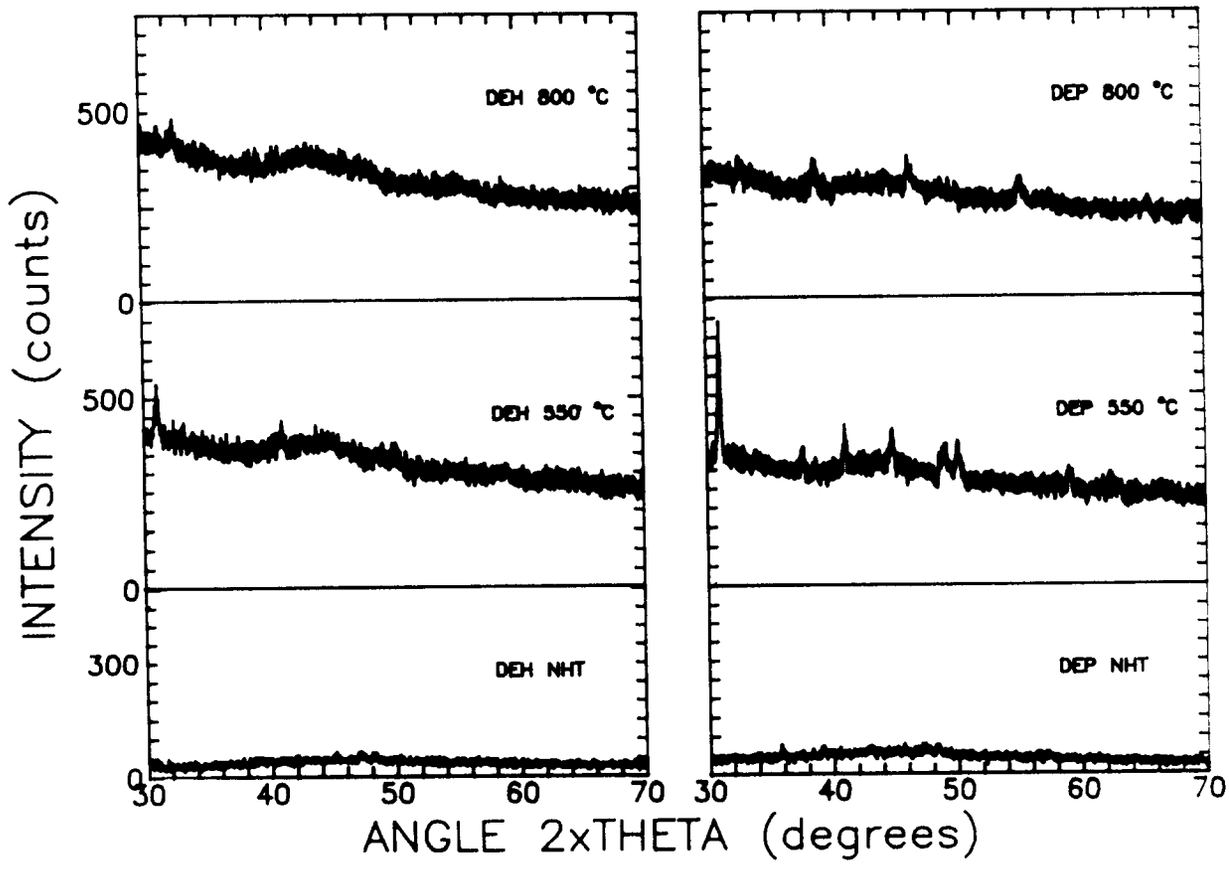

Figure 5 X-ray diffractograms of unpyrolysed DEH and DEP samples as well as of the conductive materials produced at 550 and 800°C

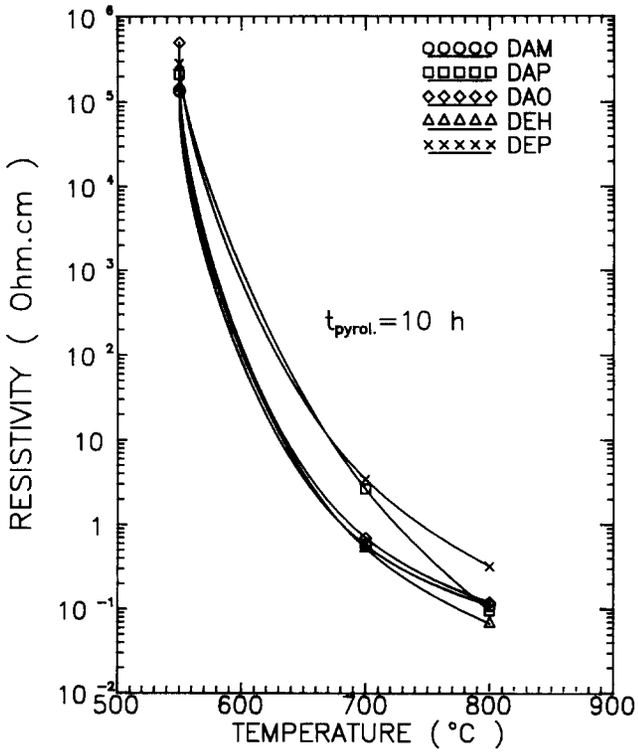

Figure 6 Electrical resistivity as a function of pyrolysis temperature of all measured conductive materials

polymers in the reactive processes of condensation and polymerization gradually lose most of their foreign atoms such as oxygen and nitrogen. Further increase in the pyrolysis temperature above 1000°C results in the entire graphitization of the materials. Thus, by increasing the pyrolysis temperature the polymers go through crystal structure changes towards the crystal structure of graphite. The low intensity of all peaks observed in *Figures 4* and *5* strongly suggests low crystallinity for all conductive materials.

The room-temperature resistance of all synthesized monomers, measured prior to pyrolysis, was found to be greater than $10^{13}\,\Omega$, which was the upper limit of the apparatus used. It is well established[14] that, in the absence of large unsaturated molecules in the unpyrolysed polymers, the energy separation from the ground level to the nearest excited energy level is large and the polymers behave practically as insulators. This is in accordance with our experimental data. All polymer precursors were then pyrolysed at 550, 700 and 800°C. During pyrolysis all samples lost weight and were converted into a black carbonaceous mass.

Figure 6 shows the electrical resistivity measured at ambient temperature of all pyrolysed conductive materials as a function of pyrolysis temperature. A dramatic decrease, almost seven orders of magnitude, in the electrical resistivity was observed as the pyrolysis temperature increased from 550 to 800°C. There is thus a systematic transition of all polymers from the behaviour of an insulator to that of a semiconductor by controlling the thermal processing temperature.

The temperature dependence of the electrical conductivity was analysed by applying two different models. According to the first, namely the variable-range hopping model, developed by Mott and Davis[20], the conductivity follows the relation:

$$\sigma = \sigma_0 \exp[-(T_0/T)^n] \quad (1)$$

where σ_0 and T_0 are parameters. The exponent n takes the values of 1/2 or 1/4, which correspond to one-dimensional and three-dimensional hopping conductivity, respectively. This model applies to amorphous materials. In spite of that, the low crystallinity of all pyrolysed conductive materials, revealed by the X-ray diffractograms, may allow the use of the model.

According to the second approach the electrical resistivity may be described by an equation of the form:

$$\rho = \rho_0 \exp[\Delta E/kT] \quad (2)$$

Equation (2) applies separately in two distinct temperature regions of the electrical resistivity (*Figures 7*, *8* and *9a*). This suggests that electrical conductivity in the samples may be attributed to two different mechanisms that are thermally activated. By applying a non-linear least-squares curve-fitting computer program, it was possible to fit the experimental data to equation (1) for $n=1/2$ and $n=1/4$ and equation (2).

Table 2 gives the values of the parameters σ_0 and T_0 for all conductive materials at various pyrolysis temperatures. *Figure 9b* shows the electrical conductivity as a function of absolute temperature for the conductive material produced by pyrolysis of DAP at 800°C for 10 h. The curves represent the fitting of the results to equation (1). It is obvious that the fitting fails to describe the experimental data in the entire temperature region.

Figures 7, *8* and *9a* present the electrical resistivity as a function of the inverse absolute temperature for all conductive materials produced by the pyrolysis of DAM and DAO, DEP and DEH, as well as of DAP, respectively, in the temperature range from −173 to 327°C (100 to 600 K). It is evident that, for each pyrolysis temperature, the electrical resistivity decreased with increasing temperature, showing two distinct temperature regions, a low-temperature and a high-temperature one, with different activation energies. This behaviour is typical for semiconductors. It has been proposed[2] that, as pyrolysis continues at higher temperatures, a continuous network of polyconjugated fused aromatic rings develops within an amorphous carbon matrix, which is formed due to a progressive carbonization among the ring systems. The increase of the pyrolysis temperature enhances the size of the conductive fused rings, allowing electric current to flow longer distances within the individual conductive species. Furthermore, it has been reported[14] that, by increasing the pyrolysis temperature up to 650°C, the electrical conduction mechanism involves the hopping of carriers through the carbon 'islands' to the next aromatic ring. When the pyrolysis temperature exceeds 700°C and progressive carbonization occurs, the conduction mechanisms change to those of graphite, namely the prevailing conduction mechanisms are those of band conduction.

Table 3 gives the values of ρ_0 and the activation energies ΔE for the two different temperature regions. It is obvious that the activation energies calculated for the high-temperature region are greater than the activation energies for the low-temperature region. These two different activation energies may be attributed to intramolecular and intermolecular charge transport,

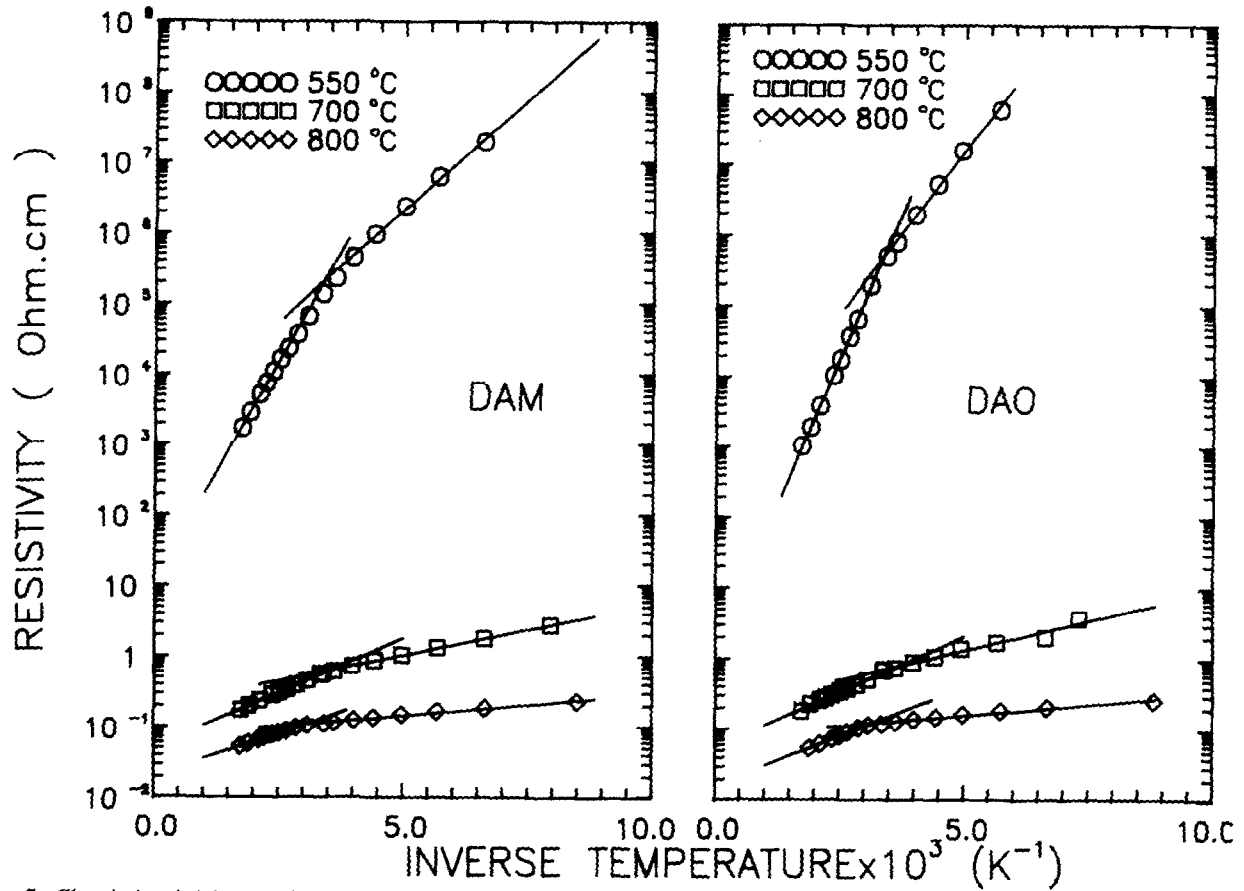

Figure 7 Electrical resistivity as a function of inverse absolute temperature of the conductive materials produced by the pyrolysis of DAM and DAO samples at 550, 700 and 800°C for 10 h

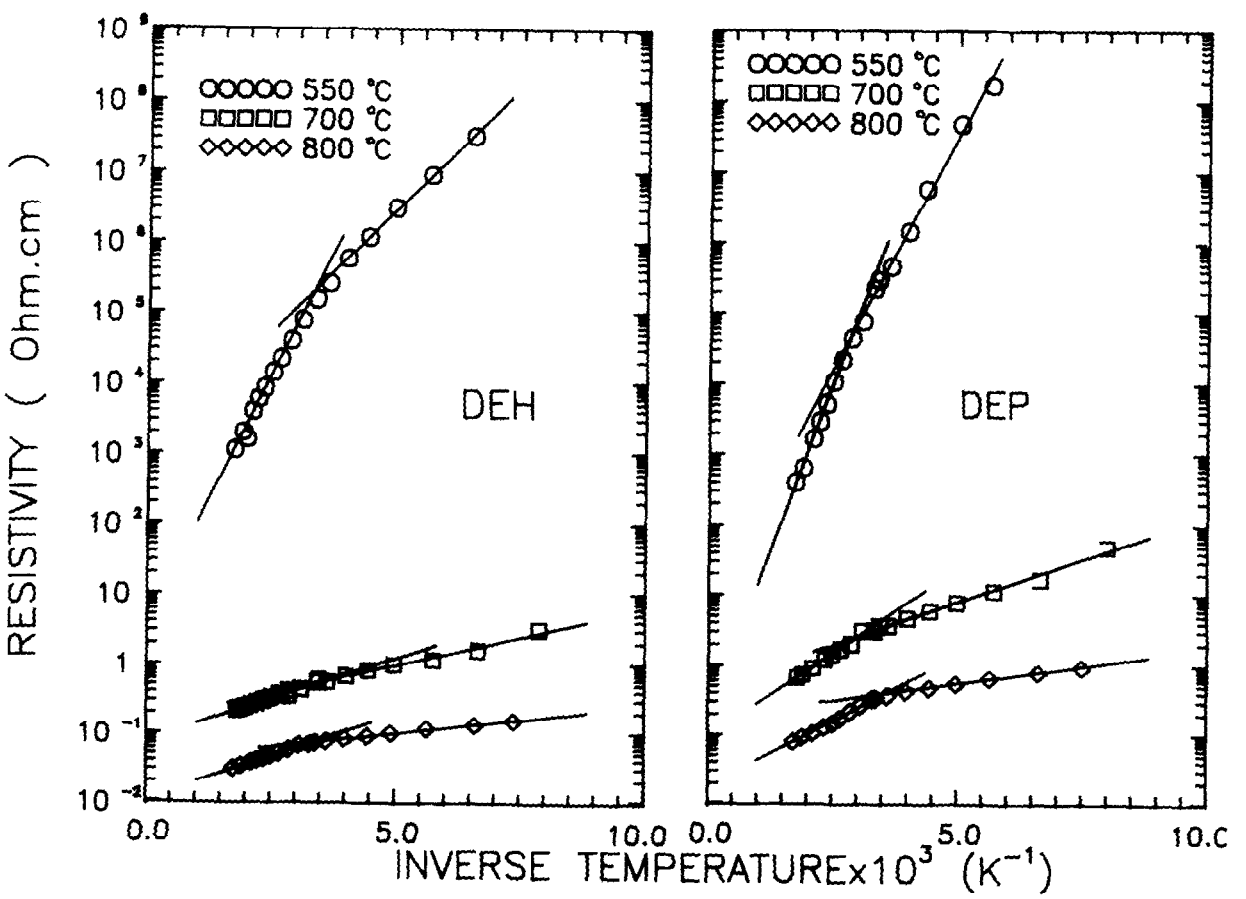

Figure 8 Electrical resistivity as a function of inverse absolute temperature of the conductive materials produced by the pyrolysis of DEP and DEH samples at 550, 700 and 800°C for 10 h

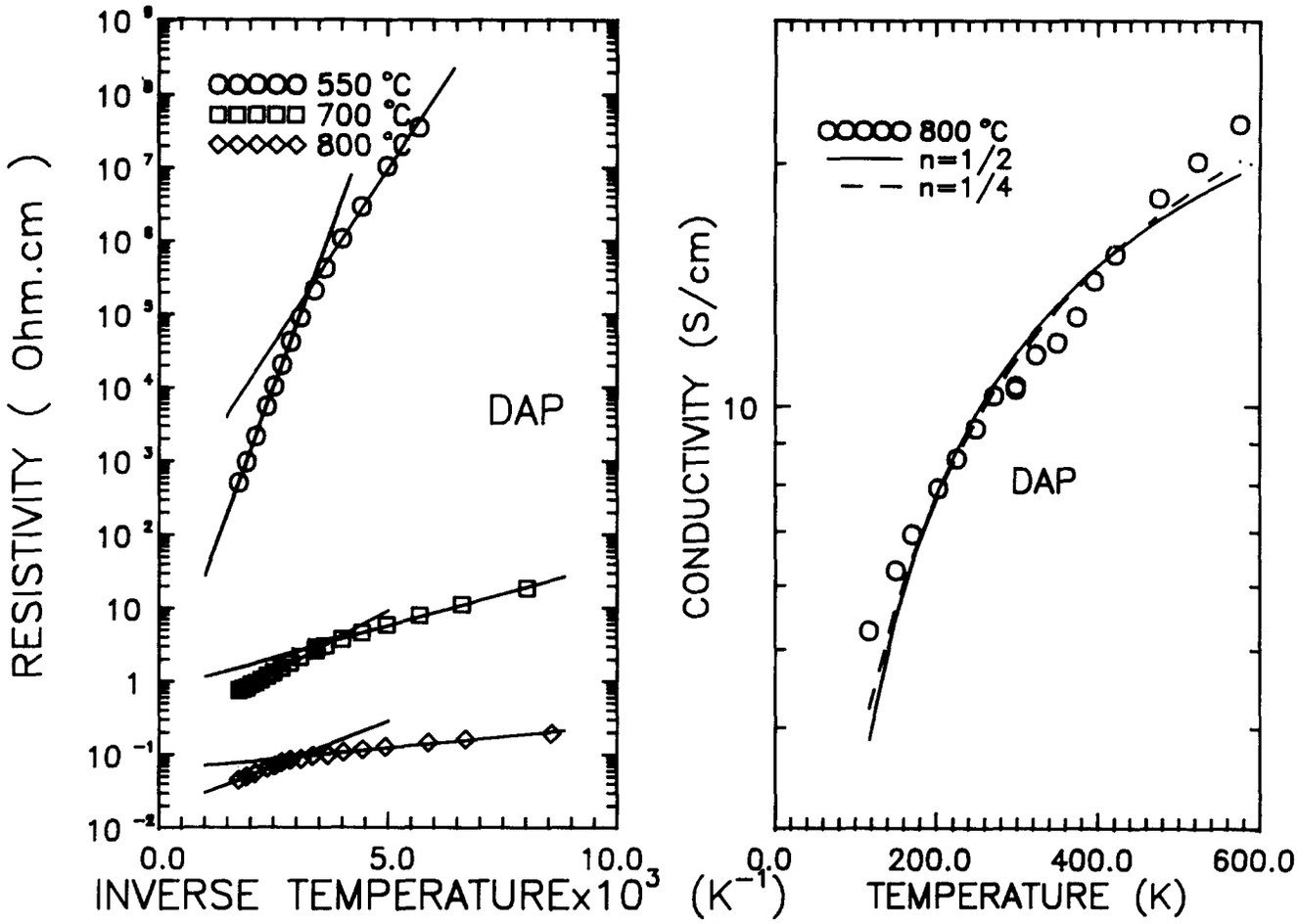

Figure 9 (a) Electrical resistivity as a function of inverse absolute temperature of the conductive materials produced by the pyrolysis of DAP samples at 550, 700 and 800°C for 10 h. (b) Non-linear least-squares fitting of the electrical conductivity of DAP pyrolysed at 800°C to relation (1) for n determined by the program, $n = 1/2$ and $n = 1/4$

Table 2 Values of parameters σ_0 and T_0 in relation (1)

Sample	Pyrolysis temperature (°C)	$n = 1/2$ σ_0 (S cm^{-1})	$n = 1/2$ T_0 (K)	$n = 1/4$ σ_0 (S cm^{-1})	$n = 1/4$ T_0 (K)
DAM	550	43.8	268.2	1.4×10^{7}	116.8
	700	76.3	62.8	2.5×10^{3}	29.8
	800	62.3	31.5	4.1×10^{2}	15.5
DAP	550	3.1×10^{22}	1.4×10^{3}	2.1×10^{30}	373.6
	700	31.4	74.4	1.7×10^{3}	34.7
	800	73.1	31.8	4.9×10^{2}	15.7
DAO	550	1.8×10^{3}	345.9	1.9×10^{10}	149.7
	700	93.7	69.5	4.3×10^{3}	32.7
	800	71.3	35.1	6.2×10^{2}	17.5
DEH	550	293.0	301.6	3.7×10^{8}	130.4
	700	51.7	55.1	1.2×10^{3}	26.4
	800	179.0	41.3	1.9×10^{3}	19.9
DEP	550	2.9×10^{4}	386.2	1.8×10^{12}	166.6
	700	73.5	91.8	9.8×10^{3}	42.5
	800	267.0	73.0	1.3×10^{4}	33.8

Table 3 Values of parameters ρ_0 and ΔE in relation (2)

Sample	Pyrolysis temperature (°C)	Low temperatures ρ_0 (Ω cm)	Low temperatures ΔE (eV)	High temperatures ρ_0 (Ω cm)	High temperatures ΔE (eV)
DAM	550	1.50×10^{3}	0.125	1.15×10^{1}	0.248
	700	1.94×10^{-1}	0.029	5.10×10^{-2}	0.061
	800	7.01×10^{-2}	0.012	2.05×10^{-2}	0.047
DAP	550	1.59×10^{2}	0.189	5.45×10^{-1}	0.338
	700	7.64×10^{-1}	0.035	1.83×10^{-1}	0.068
	800	6.10×10^{-2}	0.012	1.68×10^{-2}	0.049
DAO	550	3.78×10^{2}	0.184	1.32	0.329
	700	1.92×10^{-1}	0.033	5.49×10^{-2}	0.063
	800	7.90×10^{-2}	0.012	1.62×10^{-2}	0.056
DEH	550	9.14×10^{2}	0.139	3.86	0.280
	700	1.40×10^{-1}	0.032	7.68×10^{-2}	0.047
	800	3.37×10^{-2}	0.016	1.07×10^{-2}	0.049
DEP	550	7.32×10^{2}	0.265	1.56×10^{-1}	0.380
	700	4.32×10^{-1}	0.049	8.32×10^{-2}	0.096
	800	1.58×10^{-1}	0.020	1.58×10^{-2}	0.076

respectively. The lines in *Figures 7*, *8* and *9a* represent the fitting of the results to equation (2).

The activation energy corresponding to the low-temperature region is associated with the intermolecular conductive process, whereas the activation energy that corresponds to the high-temperature region characterizes the intramolecular conduction mechanism. It is not clear which of these two models describes the experimental data better. However, a definite conclusion could only be drawn if a molecular structure analysis could be performed.

Figures 10 and *11* show the effect of pyrolysis duration

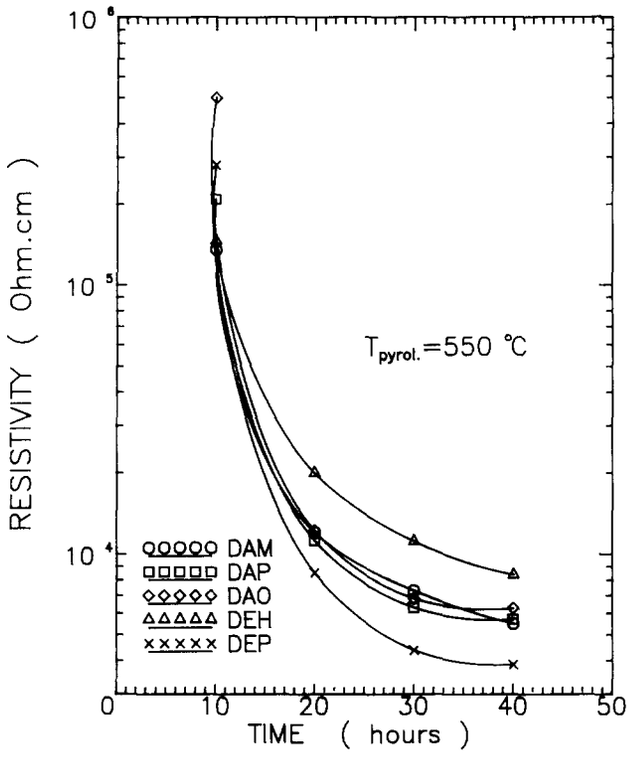

Figure 10 Electrical resistivity as a function of pyrolysis duration of all samples pyrolysed at 550°C

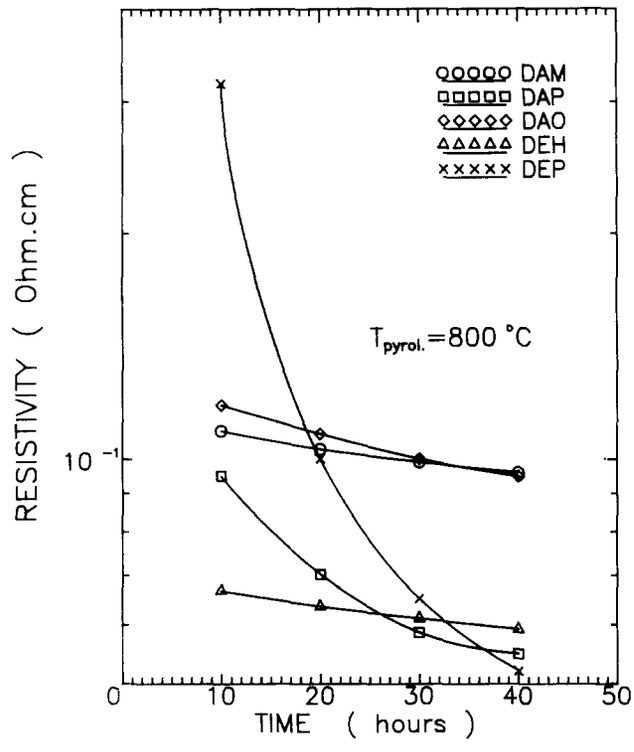

Figure 11 Electrical resistivity as a function of pyrolysis duration of all samples pyrolysed at 800°C

on the electrical resistivity of all pyrolysed conductive materials. More particularly, *Figure 10* shows the electrical resistivity of all materials pyrolysed at 550°C for 10, 20, 30 and 40 h. A dramatic increase of the electrical resistivity was observed by two orders of magnitude. As the pyrolysis duration increased, the mobility of charge carriers increased, too, owing to enhanced π-orbital overlap resulting in a decrease of the electrical resistivity. *Figure 11* reveals the electrical resistivity as a function of pyrolysis duration for all conductive materials pyrolysed at 800°C. The materials that resulted from DAM, DAO and DEH did not exhibit any significant change of their electrical resistivity. On the contrary, the materials derived from DAP and DEP still showed a considerable decrease of their electrical resistivity by almost one order of magnitude. Consequently, the latter conductive materials, which had been pyrolysed at 800°C for 40 h, exhibited the lowest attainable resistivity of $5 \times 10^{-2}\ \Omega$ cm, approximately. These values of electrical resistivity were lower than those corresponding to a pyrolysed cyano-substituted polyamide, published earlier[15], or to those corresponding to pyrolysed materials derived from the reactions of 1,4-bis(2,2-dicyanovinyl)benzene with aromatic diamines[21].

CONCLUSIONS

1-(2,2-Dicyanovinyl)-4-benzoyl chloride (DBC) was used as the starting material for the preparation of a novel class of polymer precursors. Upon heat curing, they yielded thermally stable resins, which were stable up to 333–400°C in N_2 or air and afforded anaerobic char yield of 35–60% at 800°C.

All monomers, prior to pyrolysis, behaved electrically as insulators, whereas all pyrolysed materials exhibited semiconducting behaviour. A systematic change of the electrical behaviour, from insulating to semiconducting, could be readily obtained as a function of thermal history. Inter- and intramolecular hopping conduction was rather the principal conduction mechanism.

A strong decrease of the electrical resistivity as a function of pyrolysis duration was observed at low pyrolysis temperatures. The dependence was still considerable at high pyrolysis temperatures for the materials obtained from DAP and DEP.

All polymer precursors prior to pyrolysis were amorphous, whereas all pyrolysed materials exhibited crystal structure but low crystallinity. At high pyrolysis temperatures, all materials showed multiphase structure, which could be related to their progressive graphitization.

ACKNOWLEDGEMENTS

The authors wish to express their thanks to the scientific personnel of the Inorganic and Analytical Chemistry Laboratory of the Chemical Engineering Department for their assistance in recording the X-ray diffractograms.

REFERENCES

1 Hergenrother, P. M. 'Encyclopedia of Polymer Science and Technology', Wiley, New York, 1958, Vol. 1, p. 61
2 Keller, T. M. *ChemTech* Oct. 1988, p. 635
3 Stubb, H., Punka, E. and Paloheimo, J. *Mater. Sci. Eng.* 1993, **10**, 85
4 Isotalo, H., Ahlskog, M. and Stubb, H. *Synth. Metals* 1992, **48**, 313
5 Mikroyannidis, J. A. *Eur. Polym. J.* 1991, **27**, 859
6 Mikroyannidis, J. A. *Eur. Polym. J.* 1993, **29**, 527
7 Diakoumakos, C. D. and Mikroyannidis, J. A. *Polymer* 1993, **34**, 2227
8 Mikroyannidis, J. A. *Polymer* 1994, **35**, 839

9 Mikroyannidis, J. A. *Polymer* 1994, **35**, 630
10 Mikroyannidis, J. A. *Eur. Polym. J.* in press
11 Diakoumakos, C. D. and Mikroyannidis, J. A. in press
12 Diakoumakos, C. D. and Mikroyannidis, J. A. *J. Appl. Polym. Sci.* 1994, **53**, 201
13 Mikroyannidis, J. A. *J. Polym. Sci. (A) Polym. Chem.* 1993, **31**, 1771
14 Mrozowski, S. *J. Low Temp. Phys.* 1979, **35**, 231
15 Krontiras, C. A., Pisanias, M. N., Mikroyannidis, J. A. and Georga, S. N. *Polymer* 1994, **35**, 2705
16 Takahashi, A., Suzuki, M., Suzuki, M. and Wajima, M. *J. Appl. Polym. Sci.* 1991, **43**, 943
17 Hu, C. Z. and Andrale, J. D. *J. Appl. Polym. Sci.* 1985, **30**, 4409
18 Inganas, O., Salaneck, W. R., Osterholm, J. E. and Laakso, J. *Synth. Metals* 1988, **22**, 395
19 Inganas, O., Salaneck, W. R., Osterholm, J. E. and Laakso, J. *Synth. Metals* 1988, **28**, c377
20 Mott, N. F. and Davis, E. A. 'Electronic Processes in Non-Crystalline Materials', Clarendon Press, Oxford, 1979
21 Diakoumakos, C. D., Mikroyannidis, J. A., Krontiras, C. A. and Pisanias, M. N. *J. Polym. Sci. (A) Polym. Chem.* 1994, **32**, 1915